Environmental Science & Technology

Article

pubs.acs.org/est

Effects and Location of Coplanar and Noncoplanar PCB in a Lipid Bilayer: A Solid-State NMR Study

Christian Totland,*[,†] Willy Nerdal,[†] and Signe Steinkopf[‡]

[†]Department of Chemistry, University of Bergen, Norway, Allégaten 41, N-5007 Bergen, Norway

[‡]Department of Biomedical Laboratory Sciences and Chemical Engineering, Bergen University College, 5020 Bergen, Norway

Supporting Information

ABSTRACT: Coplanar and noncoplanar polychlorinated biphenyls (PCBs) are known to have different routes and degree of toxicity. Here, the effects of noncoplanar PCB 52 and coplanar PCB 77 present at 2 mol % in a model system consisting of POPC liposomes (50% hydrated) are investigated by solid-state ^{13}C and ^{31}P NMR at 298 K. Both PCBs intercalate horizontally in the outer part of the bilayer, near the segments of the acyl chain close to the glycerol group. Despite similar membrane locations, the coplanar PCB 77 shows little effect on the bilayer properties overall, except for the four nearest neighboring lipids, while the effect of PCB 52 is more dramatic. The first ~2 layers of lipids around each PCB 52 in the bilayer form a high fluidity lamellar phase, whereas lipids beyond these layers form a lamellar phase with a slight increase in fluidity compared to a bilayer without PCB 52. Further, a third high mobility domain is observed. The explanation for this is the interference of several high fluidity lamellar phases caused by interactions of PCB 52 molecules in different leaflets of the model bilayer. This causes formation of high curvature toroidal region in the bilayer and might induce formation of channels.

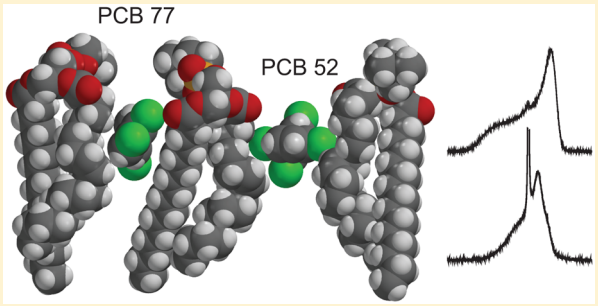

INTRODUCTION

The use of polychlorinated biphenyls (PCBs) has been highly restricted or banned in several countries since the 1970s and 1980s, although a worldwide ban was not in place until 2001.[1] However, the PCBs low biodegradability and high lipophilicity cause these compounds to accumulate in the adipose tissue of mammals as well as other creatures such as birds and fish.[2,3] Despite slow degradation, PCBs are still found in the atmosphere, even in remote locations such as Antarctica.[4] Due to the high environmental persistence and high resistance to decomposition in living organisms,[5,6] PCBs accumulate up the food chain, causing human exposure through both aquatic and terrestrial food sources. The possible effects of prolonged human exposure have therefore received considerable attention.[7]

There are as much as 209 possible configurations of PCB, where the degree and route of toxicity of various congeners varies significantly.[7] From studies of structure−activity relationships it is suggested that coplanar PCBs without chlorine substitution in the ortho position have biological properties similar to dioxin (2,3,7,8-tetrachlorobibenzo-*p*-dioxin), showing carcinogenic effects by acting on the aryl hydrocarbon receptor.[7,8] The noncoplanar PCBs, on the other hand, show different and more complex routes of toxicity, with for example estrogenic and neurotoxic activity.[9−11] Additionally, noncoplanar PCBs have shown to increase the fluidity of cellular membranes,[12−14] which may affect the activity of multiple membrane proteins.[15] Consequently, the physiological effects of noncoplanar PCBs may be far-reaching compared to coplanar PCBs.

Most previous literature focuses on effects of PCBs on cellular membranes, which illuminates effects of PCBs but makes it difficult to investigate the mechanisms of action. In order to access the core mechanisms it is helpful to utilize a model lipid membrane. PCB 77 and PCB 52 have been used in several earlier studies,[14,16,17] representing coplanar and noncoplanar PCB, respectively. Tan et al. showed that PCB 52 causes rapid cell death in thymocytes and cerebellar granule cell neurons, altering multiple membrane components, while PCB 77 showed none of these effects.[14,16] It was further shown from fluorescent polarization measurements that PCB 52 increases membrane fluidity, which was linked to the stereochemistry of the more bulky PCB 52 compared to PCB 77, causing a greater impact on membrane properties when intercalated in the bilayer structure.[16] Campbell et al. investigated interaction of these PCBs with a model 1,2-dimyristoyl-*sn*-glycero-3-phosphocholine (DMPC) lipid membrane using atomic force microscopy (ATM) and differential scanning calorimetry (DSC).[17] It was observed that bilayers with PCB 52 had a lower gel-to-liquid phase transition temperature. Additionally, fluorescence correlation spectroscopy of PCB in 1,2-dilinoleoyl-*sn*-glycero-3-phosphocholine (DLPC) fluid bilayers showed

Received: April 7, 2016
Revised: June 28, 2016
Accepted: July 5, 2016
Published: July 5, 2016

DOI: 10.1021/acs.est.6b01723
Environ. Sci. Technol. 2016, 50, 8290−8295

that PCB 52 diffuses more slowly than PCB 77 in the bilayer.[17] It was further concluded that, contrary to PCB 52, PCB 77 does not intercalate into the lipid bilayers. This latter conclusion was later questioned by Jonker and van der Heijden.[18]

In order to fully evaluate the effect and location of different PCBs in a lipid bilayer, atomic-level investigation of the bilayer is required. A technique capable of this is nuclear magnetic resonance (NMR) spectroscopy.[19−22] The amount of PCB interacting with a membrane relevant to human exposure is relatively small and remains below the detection limit of ^{13}C NMR. Still, high-resolution magic angle spinning (MAS) ^{13}C NMR can give detailed insight into the lipid-PCB interaction by monitoring changes in lipid ^{13}C spectra. Additionally, ^{31}P NMR gives direct and precise information on bilayer morphology and fluidity.[23] These techniques are applied here on a system comprising of unilamellar liposomes of POPC − a biologically abundant lipid − with and without PCB 52 or PCB 77.

The purpose of this work is to establish how noncoplanar and coplanar PCBs interact with a lipid bilayer and what possible consequences such interactions have to the bilayer properties.

MATERIALS AND METHODS

Materials. 1-Palmitoyl-2-oleoyl-*sn*-glycero-3-phosphocholine (POPC) was obtained from Avanti Polar Lipids (Birmingham, AL). PCB 52 and PCB 77 were obtained from Sigma-Aldrich.

Liposome Preparation. The amount of PCB in the samples is 2.0 mol %, which is above the limit where nonspecific toxicity occurs for noncoplanar PCB.[24] The lipid samples were dissolved in chloroform, which was then evaporated, and the samples were lyophilized overnight. The dry samples were suspended in degassed, argon bubbled water and left on a water bath for 1 h at 40 °C. In order to obtain mostly unilamellar liposomes the sample was freeze−thawed seven times using liquid N_2.[22] The samples were pH-adjusted to 7.4 by adding a small amount of 0.05 M NaOH with freezing and thawing between each adjustment. The electrolyte concentration as a result of the pH adjustment was in the order of 10^{-4} M. Samples were subjected to 24 h of lyophilization giving partially hydrated liposomes with a hydration level of ∼12 water molecules per lipid molecule.[21,22] Thus, samples with about 50 wt % water (fully hydrated lipids) could be obtained by adding degassed argon-bubbled water.[25,26] The samples were then equilibrated at 40 °C for 48 h and packed in NMR rotors in an argon-atmosphere and stored in the freezer.

NMR. The NMR data was obtained on a Bruker AV III HD 500 instrument. The instrument is equipped with magic angle spinning (MAS) hardware for 4 mm rotors (ZrO_2). Experiments were carried out at a sample temperature of 298 K. ^{13}C spectra were obtained at a sample spinning rate of 6 kHz with high-power proton decoupling during acquisition. The ^{13}C experiments were acquired with a relaxation delay of 5 s and 15000 scans. For the static ^{31}P spectra 5000 scans were collected with a relaxation delay of 3 s between transients. MAS ^{31}P experiments were carried out with a rotor spinning speed of 2.5 kHz. Simulations of static ^{31}P NMR spectra were carried out with the Topspin software (version 3.5).

RESULTS AND DISCUSSION

^{31}P NMR. Figure 1 shows the static (**A**), simulated (**B**), and MAS (**C**) ^{31}P NMR spectra of the three samples containing

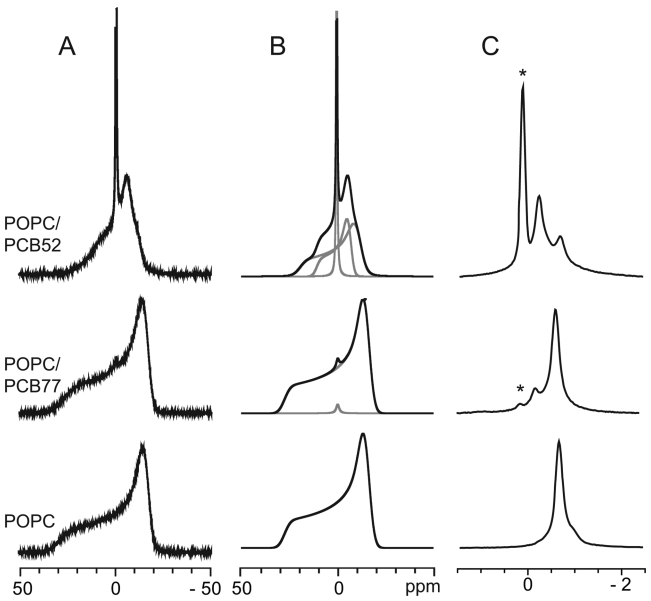

Figure 1. Recorded (**A**) and simulated (**B**) static ^{31}P NMR spectra of POPC samples (50 wt % hydration) with and without PCB 52 or 77. The central peak of corresponding MAS spectra with 2 kHz spinning are shown in **C:** An asterisk marks an isotropic high mobility phase (does not give spinning side bands), while the remaining peaks represent lamellar phases. The amount of PCB in the samples is 2 mol % relative to the lipid.

POPC, POPC + PCB 77, or POPC + PCB 52 with 50 wt % hydration. The spectrum of pure POPC shows as expected a single lamellar phase with chemical shift anisotropy (CSA) at 43 ppm. The static spectrum of the POPC+PCB 77 sample (Figure 1 **A**) shows the same lamellar phase but with a small fraction of a higher mobility isotropic phase. As seen from the simulated spectrum (Figure 1 **B**), this isotropic phase consists of a negligible fraction of POPC in the sample. It is not clear whether this isotropic phase is related to interaction with PCB 77, as a small fraction of isotropic POPC may occur during sample preparation regardless of PCB. Although not visible in the static spectrum, the corresponding MAS spectrum of the POPC + PCB 77 sample (Figure 1 **C**) shows the presence of a small additional lamellar phase, corresponding to 8.5% of the sample lipids. This lamellar phase is not observed in the static spectrum due to low abundance. If this lamellar phase is related to lipids interacting with PCB 77, it corresponds to about four affected lipids per PCB 77 molecule.

However, changes in POPC morphology in the presence of PCB 52 are clearly seen in the ^{31}P spectra (Figure 1), where a high-mobility phase is indicated by a sharp peak in the static spectrum (Figure 1 **A** and **B**), which is typical for a micellar-like phase. This phase corresponds to 18% of sample lipids. In addition, there are two lamellar phases with greater fluidity than that observed for the POPC and POPC+PCB 77 samples. The CSAs of the two lamellar phases with 2 mol % PCB 52 present are 31 and 17 ppm, representing 50% and 32% of sample lipids, respectively. The CSA value is inversely proportional to both the axial rotation of the lipids and the degree of lipid oscillation. Hence, higher lipid mobility or larger angle of the oscillation

DOI: 10.1021/acs.est.6b01723
Environ. Sci. Technol. 2016, 50, 8290−8295

will induce higher bilayer fluidity and cause lower CSA values. This indicates increased fluidity compared to the lower mobility lamellar phase observed in the POPC and POPC+PCB 77 samples (CSA = 43 ppm).

The ^{31}P NMR data confirm results from earlier studies on both cellular and model lipid bilayer samples where the presence of PCB 52 is found to increase bilayer fluidity.[14,17,26] Similar to previous studies, PCB 77 do not significantly affect the membrane fluidity; however, 4 lipids per PCB 77 adopt a lamellar phase with slightly different properties. The nature of the lipid morphologies is discussed in a separate section.

^{13}C NMR. There have been controversies regarding the localizations of PCB 52 and 77 with respect to the bilayer. It has previously been proposed that PCB 77 does not intercalate between the lipid molecules and only interacts with the headgroup,[17] something that was later argued as unlikely due to the lipophilic nature of PCB.[18] In this section the locations of PCB 52 and 77 are determined by ^{13}C NMR.

Figures 2 and 3 show the effect of PCB intercalation in the POPC bilayer. Compared to the reference sample with only

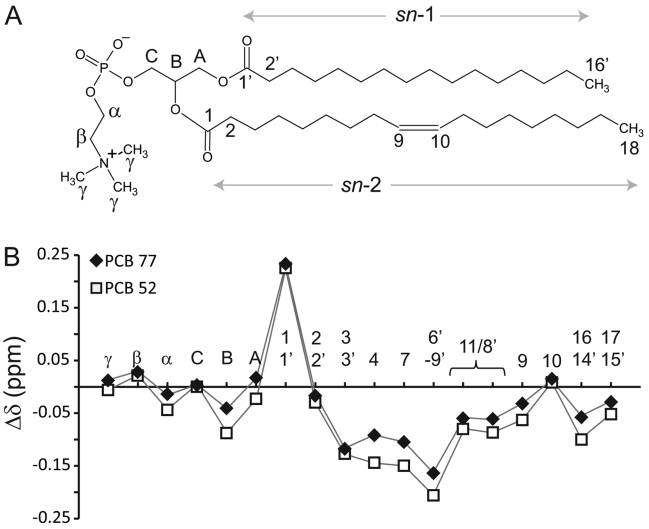

Figure 2. **A**: Molecular structure of POPC. **B**: Differences in ^{13}C chemical shifts ($\Delta\delta$) of the POPC lamellar phase in the presence of PCB 77 (◆) and PCB 52 (□), compared to a sample of POPC only. A positive value of $\Delta\delta$ means that the peak in question shifts to higher ppm values in the presence of PCB ($\Delta\delta = \delta_{w/PCB} - \delta_{POPC}$). The molecular structure of POPC is shown with labeling of the carbons according to the assignment in the plot and in Figure 3 and Figure S1 and S2 of the Supporting Information.

POPC, the ^{13}C chemical shifts of lamellar POPC are altered in samples containing PCB 77 or PCB 52 (Figure 2 B). From the plot of chemical shift differences in Figure 2, two main observations are made. First, the pattern of chemical shift differences is similar for both the PCB 52 and PCB 77 sample. However, the changes in chemical shift are slightly larger for the PCB 52 sample. Second, the changes in chemical shift are more pronounced for the carbonyl carbons (1′, 1) and subsequent acyl chain carbons. This indicates both that PCB 52 and 77 intercalate at the same position in the POPC bilayer and that this position is below the POPC carbonyl where POPC carbons in general experience a more crowded chemical environment, as evident from the decrease in chemical shift.

The displacement of the carbonyl resonance to higher chemical shift values (Figure 3 **A**) reflects a conformational

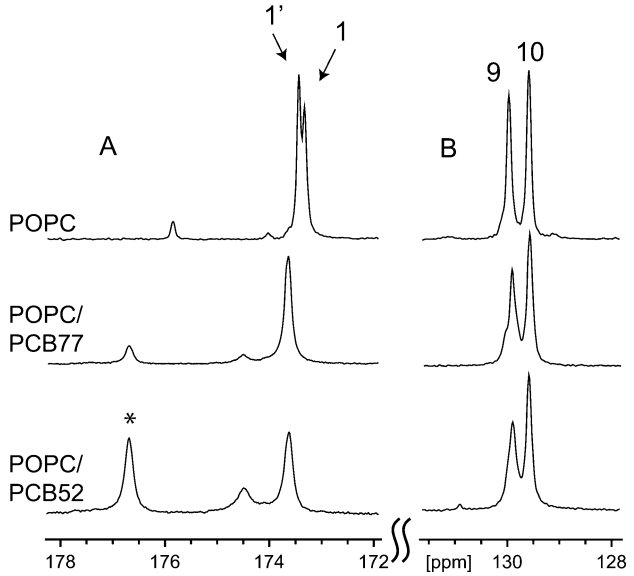

Figure 3. ^{13}C MAS NMR spectra of the carbonyl (**A**) and C═C (**B**) regions of the POPC (top), POPC + PCB 77 (middle), and POPC + PCB 52 (bottom) samples at 298 K with 50 wt % hydration. Peak labels are in accordance with the molecular structure given in Figure 2. The amount of PCB in the sample is 2 mol % relative to the lipid. The peak labeled with an asterisk is interpreted as POPC in a different phase. Assignments are based on ref 27.

change where the angle between the acyl chain and headgroup increases upon intercalation of PCB. The increased angle reduces stearic interactions between the carbonyl carbon and surrounding nuclei which in turn reduces the chemical shift. An accuracy of <0.02 ppm can be expected when internal shift referencing is used. The more pronounced shift differences (~0.5 ppm) observed for some resonances in the PCB 52 sample, for example acyl chain carbons 4 and 7 (Figure 2 B), is most likely due to the higher angle between the phenyl planes and consequent more bulky stereochemistry of PCB 52 compared to PCB 77. As discussed in the next section, the ^{31}P NMR results suggest that this difference causes PCB 52 to affect lipids in a greater radius compared to PCB 77.

For the model POPC bilayer, the location of PCB below the carbonyl segments and above carbon number 9 from the carbonyl of the acyl chains is further illustrated by the C═C resonances shown in Figure 3 **B**. Here, carbon 9, which is closest to the headgroup, is clearly affected by the presence of both PCB 52 and 77, while carbon 10 remains unaffected. These results suggest that the PCB molecules are oriented with the long molecular axis horizontally to the bilayer plane, as a vertical orientation would be expected to affect ^{13}C resonances further down the acyl chains. The small dipole moments present when the phenyl plane configurations are as in Figure 4 **A** can then be oriented with the positive part toward the negative charge of the POPC headgroup. The resulting PCB orientations are shown schematically in Figure 4 **B** for this scenario. However, dynamics such as rotational averaging of the PCB and lipid molecules are not considered in the figure.

Another notable feature in the ^{13}C spectra is the appearance of additional POPC peaks, particularly in the PCB 52 sample. This is shown in Figure 3 **A** for the carbonyl spectral region. The origins of these peaks are various POPC morphologies in the PCB 52 sample that are not present to a significant extent in the absence of PCB 52. The small additional peaks seen in

DOI: 10.1021/acs.est.6b01723
Environ. Sci. Technol. 2016, 50, 8290−8295

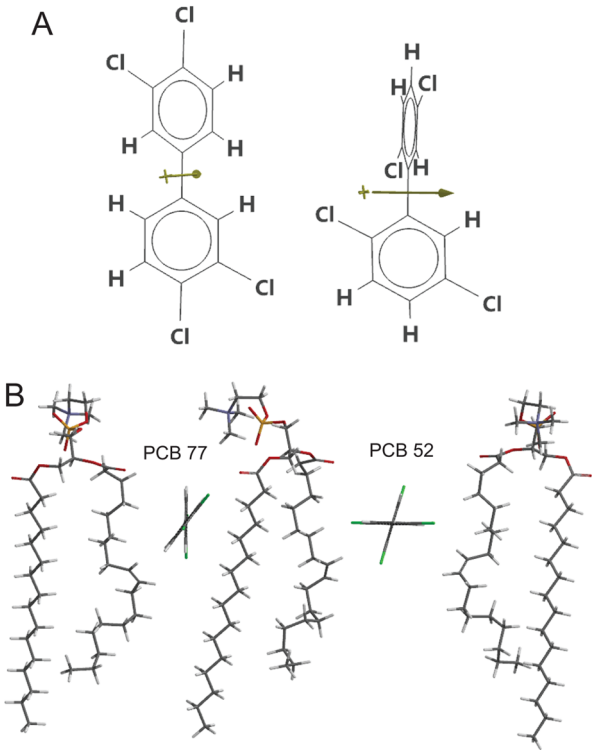

Figure 4. A: PCB77 (left) and PCB52 (right). The stereochemistry is calculated by the use of density functional theory (Spartan '14). The torsion angles between phenyl planes for the shown configurations are ~76° for PCB52 and ~37° for PCB77. These configurations correspond to dipole moments of 0.28 and 0.86 D, respectively (directions indicated). Note however that dipole moments will vary as the phenyl rings twist.[18] **B**: Schematic side view of PCB 77 and 52 intercalated in a POPC layer, showing the more bulky stereochemistry of PCB 52.

the carbonyl and headgroup regions of the POPC and POPC + PCB 77 ^{13}C spectra are likely related to the sample packing, where bilayer regions with extended curvature can occur in the turns of flattened liposomes and at the sample-rotor interface. The ^{31}P NMR spectra (Figure 1) confirm the presence of different morphological states of POPC in the PCB 52 sample. The morphology of aggregated amphiphilic molecules has potentially a large impact on the molecules' ^{13}C chemical shifts, particularly those of the headgroup region. For example, ^{13}C resonances from carbons near the headgroup region of tetradecyltrimethylammonium bromide increase as much as 1.5 ppm upon transition from bilayer to micelle.[28] Therefore, the additional carbonyl peak at higher ppm values in the PCB 52 sample (Figure 3) most likely correlates to the high mobility micellar-like phase seen in the ^{31}P spectrum. Additional peaks also appear around other resonances from carbons near the headgroup region, including the glycerol (A, B, and C) and cholin (γ, α, and β) carbons, as well as the first three carbons of the acyl chains (1, 1′−3, 3′) (see the Supporting Information).

Lipid Morphologies in the PCB 52 and PCB 77 Samples. The changes in bilayer morphology and fluidity in the presence of PCB 52 are related to stearic interactions between the POPC acyl chain and PCB 52. With 2 mol % PCB 52, the most notable changes in bilayer morphology are a high fluidity lamellar phase constituting 32% of sample lipids and a high mobility micellar-like phase constituting 18% of sample lipids. As mentioned, the remaining lipids form a less mobile lamellar phase, which still has higher fluidity than the single lamellar phase seen in the POPC+PCB 77 and POPC samples (Figure 1).

The sample contains 2 mol % PCB 52 relative to the amount of lipid. A reasonable assumption is that PCB 52 has highest impact on nearest and next nearest neighboring lipids and that the most mobile of the lamellar phases relates to these regions. Further, if PCB 52 molecules localized in separate leaflets of the bilayer become close in space, the mobile lamellar phases of both leaflets will interact and destabilize the bilayer. The result of this interaction is formation of a curved toroidal region which will resemble a micellar-like phase in the NMR spectra and facilitate formation of channels in the bilayer. The location of PCB 52 close to the choline headgroup will increase the headgroup cross-sectional area relative to the acyl chain. This gives a packing parameter that facilitates increased curvature, similar to a micellar phase, when several PCB 52s are near each other at both sides of the bilayer. Conversely, a PCB location closer to the core of the bilayer could reduce the curvature and cause inverse hexagonal phases when multiple PCB 52s interact in the bilayer. Such inverse hexagonal phases result in powder pattern ^{31}P resonances which are not seen here. Hence, the presence of a micellar-like phase supports that PCB locates in the outer part of the bilayer hydrophobic core. A schematic presentation of the bilayer is illustrated in Figure 5 where the

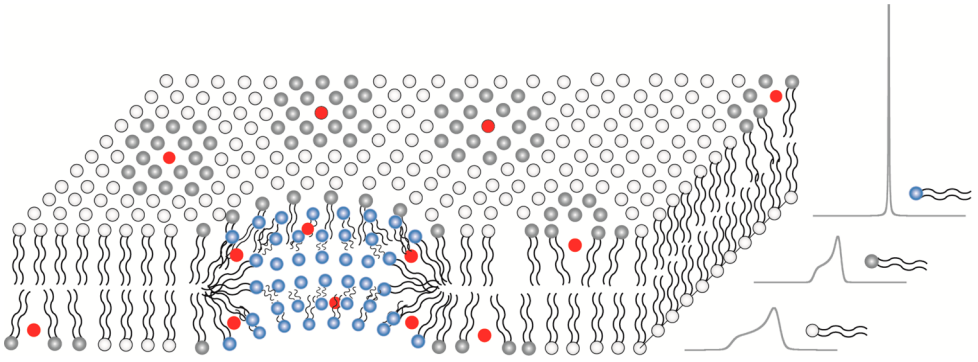

Figure 5. Schematic view of the POPC bilayer with intercalated PCB 52, illustrating the three POPC phases observed from the ^{31}P spectra with 2 mol % PCB 52. The simulated ^{31}P spectra of the various phases are shown (from Figure 1 B). White orbs represent the less mobile lamellar phase (50%), gray orbs represent the mobile lamellar phase (32%), and blue orbs represent the curved toroidal/micellar phase (18%). The intercalated PCB 52 molecules (2%) are represented as red orbs. The number of orbs representing each phase approximately equals the fraction percentage found by ^{31}P NMR and thus gives a realistic distribution of the phases and PCB 52 in the bilayer.

DOI: 10.1021/acs.est.6b01723
Environ. Sci. Technol. 2016, 50, 8290−8295

micellar phase is represented as a curved toroidal region which forms a channel in the bilayer.

The data presented here gives molecular-level details about the interaction of coplanar and noncoplanar PCBs with a lipid bilayer, beyond what has been shown earlier. Particularly, the ability of noncoplanar PCB 52 to potentially disrupt the bilayer upon formation of curved toroidal regions may explain the cytotoxic effects of these chemicals.[14] Moreover, the interaction of the high fluidity lamellar phase occurring around each PCB 52 with membrane proteins will significantly affect protein function, as observed earlier.[12−15]

In the schematic bilayer representations shown in Figure 5 it is indicated that where a large enough number of PCB 52 molecules can be found in a limited region, the POPC bilayer will collapse and form a micellar-like phase. The POPC lipids in such a phase can be expected to return to bilayer when the PCB molecules that cause the micellar phase diffuse apart and that these processes will move around in the POPC bilayer depending on the number of PCB molecules found in a limited region. It should be noted that this study is conducted at a single PCB concentration using a model POPC bilayer. In a biological system other toxicological mechanisms may come into play at various concentrations; however, at the current PCB bilayer concentration the high fluidity phase occurring about each PCB 52 likely has highly adverse effects, also in a biological system.

The results show that PCB 77 does not affect membrane properties significantly, despite a similar location to PCB 52. However, the ^{31}P MAS NMR spectra suggests that PCB 77 in fact does have an effect on neighboring lipids which form a higher mobility lamellar phase similar to the one observed in the PCB 52 sample, due to the similar isotropic ^{31}P chemical shifts. The difference is the extent of the effect, where one PCB 77 affects about 4 lipids and one PCB 52 affect 16 lipids, likely due to the different stereochemistry of the two PCBs. The small effect of PCB 77 will not be detectable by techniques used in previous studies and was e.g. misinterpreted in an earlier study by Campbell et al. to suggest that PCB 77 does not intercalate in the bilayer.[17]

When utilizing a model lipid membrane, the biological relevance of the model system is of importance in order to translate the effects to biological systems. Here, the biological abundant POPC is used, which means that general properties of the bilayer, such as thickness and chain saturation, resemble a cellular membrane. In particular, the formation of curved toroidal regions may depend on such bilayer properties. Still, the results presented here display many of the same trends as previous studies using more typical saturated model lipids such as 1,2-dipalmitoyl-*sn*-glycero-3-phosphoch (DPPC),[14] DMPC, and DLPC,[17] where increased fluidity in the presence of PCB 52 is observed. PCB 52 is found to be among the more abundant PCB congeners in both animals and in the atmosphere,[3,4] making knowledge about its toxicological routes important.

■ ASSOCIATED CONTENT

Supporting Information

The Supporting Information is available free of charge on the ACS Publications website at DOI: 10.1021/acs.est.6b01723.

^{13}C spectra (all spectral regions); ^{31}P MAS spectra; Figures S1−S5; reference S1 (PDF)

■ AUTHOR INFORMATION

Corresponding Author

*Phone: +47 55588233. E-mail: christian.totland@uib.no.

Author Contributions

The manuscript was written through contributions of all authors. All authors have given approval to the final version of the manuscript.

Notes

The authors declare no competing financial interest.

■ ACKNOWLEDGMENTS

We would like to acknowledge Dr.scient. Sonnich Meier, Institute of Marine Research, Bergen, Norway and Prof. Knut Teigen, The Department of Biomedicine, University of Bergen, Norway for providing some of the sample material used.

■ ABBREVIATIONS

POPC	1-palmitoyl-2-oeloylphosphatidylcholine
DMPC	dimyristoylphosphatidylcholine
DPPC	dipalmitoylphosphatidylcholine
PCB	polychlorinated biphenyls
NMR	nuclear magnetic resonance
MAS	magic angle spinning

■ REFERENCES

(1) Porta, M.; Zumeta, E. Implementing the Stockholm Treaty on Persistent Organic Pollutants. *Occup. Environ. Med.* **2002**, *59* (10), 651−652.

(2) McFarland, V. A.; Clarke, J. U. Environmental occurrence, abundance, and potential toxicity of polychlorinated biphenyl congeners: considerations for a congener-specific analysis. *Environ. Health Perspect.* **1989**, *81*, 225−239.

(3) Dorneles, P. R.; Lailson-Brito, J.; Secchi, E. R.; Dirtu, A. C.; Weijs, L.; Dalla Rosa, L.; Bassoi, M.; Cunha, H. A.; Azevedo, A. F.; Covaci, A. Levels and profiles of chlorinated and brominated contaminants in Southern Hemisphere humpback whales, Megaptera novaeangliae. *Environ. Res.* **2015**, *138*, 49−57.

(4) Kallenborn, R.; Breivik, K.; Eckhardt, S.; Lunder, C. R.; Manø, S.; Schlabach, M.; Stohl, A. Long-term monitoring of persistent organic pollutants (POPs) at the Norwegian Troll station in Dronning Maud Land, Antarctica. *Atmos. Chem. Phys.* **2013**, *13* (14), 6983−6992.

(5) von Waldow, H.; MacLeod, M.; Jones, K.; Scheringer, M.; Hungerbühler, K. Remoteness from emission sources explains the fractionation pattern of polychlorinated biphenyls in the northern hemisphere. *Environ. Sci. Technol.* **2010**, *44* (16), 6183−6188.

(6) Beyer, A.; Biziuk, M. Environmental fate and global distribution of polychlorinated biphenyls. *Rev. Environ. Contam. Toxicol.* **2009**, *201*, 137−158.

(7) Carpenter David, D. O. Polychlorinated Biphenyls (PCBs): Routes of exposure and effects on human health. *Rev. Environ. Health* **2006**, *21*, 1.

(8) Safe, S. H. Polychlorinated biphenyls (PCBs): environmental impact, biochemical and toxic responses, and implications for risk assessment. *Crit. Rev. Toxicol.* **1994**, *24* (2), 87−149.

(9) Arnold, D. L.; Mes, J.; Bryce, F.; Karpinski, K.; Bickis, M. G.; Zawidzka, Z. Z.; Stapley, R. A pilot study on the effects of Aroclor 1254 ingestion by rhesus and cynomolgus monkeys as a model for human ingestion of PCBs. *Food Chem. Toxicol.* **1990**, *28* (12), 847−857.

(10) Saint-Amour, D.; Roy, M.-S.; Bastien, C.; Ayotte, P.; Dewailly, É.; Després, C.; Gingras, S.; Muckle, G. Alterations of visual evoked potentials in preschool Inuit children exposed to methylmercury and polychlorinated biphenyls from a marine diet. *NeuroToxicology* **2006**, *27* (4), 567−578.

DOI: 10.1021/acs.est.6b01723
Environ. Sci. Technol. 2016, 50, 8290−8295

(11) Fischer, L. J.; Seegal, R. F.; Ganey, P. E.; Pessah, I. N.; Kodavanti, P. R. Symposium overview: toxicity of non-coplanar PCBs. *Toxicol. Sci.* **1998**, *41* (1), 49−61.
(12) Bonora, S.; Torreggiani, A.; Fini, G. DSC and Raman study on the interaction between polychlorinated biphenyls (PCB) and phospholipid liposomes. *Thermochim. Acta* **2003**, *408* (1−2), 55−65.
(13) Gonzalez, A.; Odjélé, A.; Weber, J.-M. PCB-153 and temperature cause restructuring of goldfish membranes: Homeoviscous response to a chemical fluidiser. *Aquat. Toxicol.* **2013**, *144−145*, 11−18.
(14) Tan, Y.; Chen, C. H.; Lawrence, D.; Carpenter, D. O. Ortho-substituted PCBs kill cells by altering membrane structure. *Toxicol. Sci.* **2004**, *80* (1), 54−59.
(15) Šimečková, P.; Vondráček, J.; Procházková, J.; Kozubík, A.; Krčmář, P.; Machala, M. 2,2′,4,4′,5,5′-Hexachlorobiphenyl (PCB 153) induces degradation of adherens junction proteins and inhibits *β*-catenin-dependent transcription in liver epithelial cells. *Toxicology* **2009**, *260* (1−3), 104−111.
(16) Tan, Y.; Li, D.; Song, R.; Lawrence, D.; Carpenter, D. O. Ortho-substituted PCBs kill thymocytes. *Toxicol. Sci.* **2003**, *76* (2), 328−337.
(17) Campbell, A. S.; Yu, Y.; Granick, S.; Gewirth, A. A. PCB association with model phospholipid bilayers. *Environ. Sci. Technol.* **2008**, *42* (19), 7496−7501.
(18) Jonker, M. T. O.; van der Heijden, S. A. Comment on "PCB association with model phospholipid bilayers. *Environ. Sci. Technol.* **2009**, *43* (13), 5155−5156.
(19) Grélard, A.; Loudet, C.; Diller, A.; Dufourc, E. J. NMR spectroscopy of lipid bilayers. In *Membrane Protein Structure Determination: Methods and Protocols*; Lacapère, J.-J., Ed.; Humana Press: Totowa, NJ, 2010; pp 341−359.
(20) Bonev, B. B. Chapter Eleven - High-Resolution Solid-State NMR of Lipid Membranes. In *Advances in Planar Lipid Bilayers and Liposomes*; Aleš, I., Julia, G., Eds.; Academic Press: 2013; Vol. Vol. *17*, pp 299−329.
(21) Song, C.; Holmsen, H.; Nerdal, W. Existence of lipid microdomains in bilayer of dipalmitoyl phosphatidylcholine (DPPC) and 1-stearoyl-2-docosahexenoyl phosphatidylserine (SDPS) and their perturbation by chlorpromazine: a ^{13}C and ^{31}P solid-state NMR study. *Biophys. Chem.* **2006**, *120* (3), 178−187.
(22) Nerdal, W.; Gundersen, S. A.; Thorsen, V.; Høiland, H.; Holmsen, H. Chlorpromazine interaction with glycerophospholipid liposomes studied by magic angle spinning solid state ^{13}C-NMR and differential scanning calorimetry. *Biochim. Biophys. Acta, Biomembr.* **2000**, *1464* (1), 165−175.
(23) Picard, F.; Paquet, M.-J.; Levesque, J.; Bélanger, A.; Auger, M. ^{31}P NMR first spectral moment study of the partial magnetic orientation of phospholipid membranes. *Biophys. J.* **1999**, *77* (2), 888−902.
(24) van Wezel, A. P.; Opperhuizen, A. Narcosis due to environmental pollutants in aquatic organisms: Residue based toxicity, mechanisms and membrane burdens. *Crit. Rev. Toxicol.* **1995**, *25* (3), 255−279.
(25) Janiak, M. J.; Small, D. M.; Shipley, G. G. Temperature and compositional dependence of the structure of hydrated dimyristoyl lecithin. *J. Biol. Chem.* **1979**, *254* (13), 6068−6078.
(26) Small, D. M. Phase equilibria and structure of dry and hydrated egg lecithin. *J. Lipid Res.* **1967**, *8* (6), 551−557.
(27) Ferreira, T. M.; Coreta-Gomes, F.; Ollila, O. H.; Moreno, M. J.; Vaz, W. L.; Topgaard, D. Cholesterol and POPC segmental order parameters in lipid membranes: solid state ^{1}H-^{13}C NMR and MD simulation studies. *Phys. Chem. Chem. Phys.* **2013**, *15* (6), 1976−1989.
(28) Totland, C.; Nerdal, W. Thermotropic behavior of a cationic surfactant in the adsorbed and micellar state: An NMR study. *Langmuir* **2012**, *28* (16), 6569−6576.

DOI: 10.1021/acs.est.6b01723
Environ. Sci. Technol. 2016, 50, 8290−8295